note that the effective fields in (25) depend only on differences of displacements, and therefore lead to force terms of the same form as the short-range "elastic" interactions. Thus the equations of motion of the lattice[16] will be unchanged, and the only effect of the corrections we have found to the Lorentz effective field will be to change the interpretation of some of the coefficients in the equations of motion for the long-wavelength optical modes.

Effective fields for waves of arbitrary wavelength have recently been considered by Cochran.[17] His results are for rigid ions but, if modified to allow for separate displacements of the core and one or more electron shells, they are equivalent in the long-wavelength limit to the results given here.

ACKNOWLEDGMENTS

We are grateful to the Naval Ordnance Laboratory, where this work was begun, for its support. We also thank Dr. Arnold H. Kahn of the National Bureau of Standards for his interest in this work, and Dr. Robert W. Keyes for comments on the manuscript.

[16] See, for example, Eq. (3.2) of W. Cochran, in *Advances in Physics*, edited by B. H. Flowers (Taylor and Francis, Ltd. London, 1960), Vol. 9, p. 387.

[17] W. Cochran, Proc. Roy. Soc. (London) **A276**, 308 (1963); Proceedings of the International Conference on Lattice Dynamics, Copenhagen, 1963 (to be published). We are indebted to Dr. Cochran for sending us his results prior to publication.

PHYSICAL REVIEW VOLUME 134, NUMBER 2A 20 APRIL 1964

Spin-Wave Renormalization Applied to Ferromagnetic $CrBr_3$†

H. L. Davis* and Albert Narath
Sandia Laboratory, Albuquerque, New Mexico
(Received 18 November 1963)

Nuclear-magnetic-resonance-domain magnetization data for ferromagnetic $CrBr_3$ have been extended over the range 1–20°K. Using the low-temperature ($\leq$5.25°K) data and Holstein-Primakoff spin-wave theory without the usual long-wavelength approximation, we have shown that exchange constants reported by Gossard, Jaccarino, and Remeika are in error by about 40%. This error resulted from the long-wavelength approximation, which causes, even at temperatures $\frac{1}{8}$th the Curie temperature, errors much larger than experimental errors. In the low-temperature range, we have found a 20% range for the values of the exchange constants which will explain the experimental results. However, by using spin-wave renormalization techniques to interpret the intermediate temperature data, the acceptable range in values for the exchange constants is narrowed to less than 2%. We have been able to fit the experimental NMR frequencies, throughout the temperature range of 1–20°K, with the renormalized spin-wave theory. The resulting rms error of 16.2 kc/sec lies within the mean experimental error, thereby giving experimental verification to the approximations used in developing the spin-wave renormalization. This data fit gives 8.25°K for the intralayer exchange constant, 0.497°K for the interlayer exchange constant, and 58.099 Mc/sec for the 0°K, zero-field Cr^{53} resonance frequency.

I. INTRODUCTION

CONSIDERABLE interest has been shown in recent years in comparisons of experimental results with predictions of the Heisenberg model of magnetism; e.g., measurements of the magnetization of a variety of magnetically ordered crystals have been made and the results interpreted by spin-wave theories of varying degrees of sophistication.[1] In particular, two nuclear-magnetic-resonance (NMR) magnetization measurements and their interpretations have a bearing on the present investigation: (1) The work of Gossard, Jaccarino, and Remeika[2] (hereafter referred to as GJR) on ferromagnetic $CrBr_3$, and (2) the work of Narath[3] on antiferromagnetic $CrCl_3$. At low temperatures, the structures of these crystals are isomorphic,[4] and can be represented by Fig. 1 (a). In both cases, the strongest exchange coupling is the ferromagnetic coupling J_T, of nearest neighbors in the hexagonal basal plane. The interlayer exchange coupling J_L is ferromagnetic in $CrBr_3$ and antiferromagnetic in $CrCl_3$.

We have noticed an inconsistency between J_T reported for $CrBr_3$ and the one reported for $CrCl_3$; that is, for $CrCl_3$ the value $J_T/k=4.5$°K obtained via spin-wave theory is considerably larger than the one deduced from the ordering temperature T_c by means of the molecular field approximation

$$J_T/k=3T_c/[2zS(S+1)], \tag{1.1}$$

† This work performed under the auspices of the U. S. Atomic Energy Commission.

* Now at Bellcomm, Incorporated, Washington, D. C.

[1] Exhaustive references may be found in the review article of P. W. Anderson, Solid State Phys. **14**, 99 (1963).

[2] A. C. Gossard, V. Jaccarino, and J. P. Remeika, Phys. Rev. Letters **7**, 122 (1961).

[3] A. Narath, Phys. Rev. Letters **7**, 410 (1961); Phys. Rev. **131**, 1929 (1963).

[4] B. Morosin and A. Narath, J. Chem. Phys. **40**, 1958 (1964).

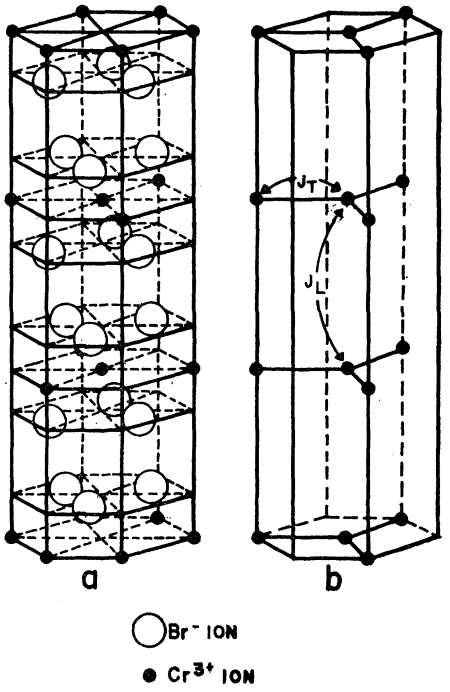

FIG. 1. (a) Crystal structure of $CrBr_3$. (b) Simplified crystal model for the Cr^{3+} ions used in the spin-wave calculations.

which gives $J_T/k=2.2°K$. However, for $CrBr_3$ the values of J_T/k obtained by the two methods are approximately the same, being 5.4 and 4.9°K, respectively. The question arises whether this discrepancy is due to fundamental differences in the physical properties of these crystals or to an incorrect analysis of the data. In the analysis of the $CrBr_3$ data the long-wavelength approximation to spin-wave theory was used without consideration of its effect, while for $CrCl_3$ the effect of such an approximation was explicitly considered and was found to have a significant influence on the value of J_T obtained from the experiment. Thus, one of the motivations for the present work was to see if the discrepancy between the J_T's could be removed by a reanalysis of the $CrBr_3$ data. We have, therefore, made a study of the factors influencing the accuracy which can be obtained in the determination of the exchange constants from a low-temperature spin-wave analysis of the experimental data. We will show in Sec. IV that a correct analysis, in fact, leads to a much larger value for J_T in $CrBr_3$ than that obtained by GJR.

A second motivation for this work has been the hope that the simple exchange Hamiltonian appropriate for $CrBr_3$ would provide a fairly straightforward experimental test for the validity of spin-wave renormalization procedures.[5–7] After reanalyzing the low-temperature data, we have therefore applied the concepts of spin-wave renormalization to an interpretation of the data obtained at intermediate temperatures where one expects the Holstein-Primakoff[8] (hereafter referred to as HP) spin-wave theory to break down because of interactions between HP spin waves. Spin-wave renormalization is an approximate method of taking into account interactions between HP spin waves by allowing the excitation energy of a given spin wave to change with temperature. As is seen in Sec. IV, an explanation of the intermediate-temperature data is possible only with renormalization, thereby providing experimental verification of the approximations used in the spin-wave renormalization. At the same time, we have considered whether a wider temperature range than HP spin-wave theory allows can yield more accurate Heisenberg exchange parameters. Again, as Sec. IV will show, this expectation is fulfilled.

In the course of the present work we have extended the Cr^{53} zero-field NMR measurements of GJR over the range 1–20°K; the experimental techniques are discussed in Sec. III. The theory required for the analysis of the data is discussed in detail in Sec. II.

II. THEORY

Although $CrBr_3$ has the $R\bar{3}$ hexagonal layer structure[9] shown in Fig. 1(a), we will follow GJR and approximate the Cr^{3+} lattice by one represented in Fig. 1(b). Such an approximation greatly reduces the effort required to derive a spin-wave dispersion law which closely resembles the true dispersion law for the magnetic collective modes of $CrBr_3$ at low temperatures; furthermore, the same approximation allows our renormalization calculation to proceed in a much more straightforward manner. Moreover, such an approximation has more justification than that of simplifying the calculations, since one expects the intralayer exchange coupling, which proceeds by means of superexchange through a single Br^- ion, to be much stronger than the interlayer exchange coupling which proceeds through two Br^- ions. This expectation has been verified by GJR who found that J_T was larger than J_L by a factor of six; as we will show, a more correct treatment of the theory gives J_T greater than J_L by a factor of 16. Thus, qualitatively, experiment and theory interact to provide some self-consistency to this approximation of the lattice. Therefore, in our theoretical treatment, we have restricted ourselves to the model of Fig. 1(b) and have considered only nearest-neighbor couplings between the spins. This model has two inequivalent spin sites per unit cell; hence, we consider a $2N$ spin system with periodic boundary conditions, composed of two sublattices of N spins each. The spin operators corresponding to the spins of one sublattice are denoted by $\mathbf{R}_k$, while those of the other sublattice are denoted by $\mathbf{S}_j$, with $|\mathbf{S}_j|=|\mathbf{R}_k|$

[5] F. Keffer and R. Loudon, J. Appl. Phys. Suppl. **32**, 2S (1961).
[6] R. Brout and F. Englert, Bull. Am. Phys. Soc. **6**, 55 (1961).
[7] M. Bloch, Phys. Rev. Letters **9**, 286 (1962).
[8] T. Holstein and H. Primakoff, Phys. Rev. **58**, 1098 (1940).
[9] Å. Braekken, Kgl. Norske Videnskab. Selskab Forh. **5**, No. 11 (1932).

$=S$. Angular momentum is measured in units of $\hbar$. Acting on each spin is an anisotropy field, denoted by H_A, which we assume to be the same at the two inequivalent sites and which is directed along the $+z$ direction.

The Hamiltonian for the above model is

$$\begin{aligned}\mathcal{H}=&-2J_T\textstyle\sum_{j,\delta}\mathbf{S}_j\cdot\mathbf{R}_{j+\delta}\\&-J_L(\textstyle\sum_{j,\delta'}\mathbf{S}_j\cdot\mathbf{S}_{j+\delta'}+\sum_{k,\delta'}\mathbf{R}_k\cdot\mathbf{R}_{k+\delta'})\\&-g\mu_BH_A(T)(\textstyle\sum_j S_j{}^z+\sum_k R_k{}^z),\end{aligned}\quad(2.1)$$

where $\boldsymbol{\delta}$ denotes the vectors from a given spin site to nearest-neighbors in the same layer, and $\boldsymbol{\delta}'$ denotes the vectors to nearest-neighbors in adjacent layers. The first sum of (2.1) describes the intralayer Heisenberg exchange coupling between nearest neighbors; the second and third sums describe the interlayer coupling between nearest neighbors in adjacent layers; and the last two sums account for the anisotropy. We have explicitly written the anisotropy as a function of the temperature T for the following reasons. Spin waves are only approximate collective modes for an exchange-coupled spin system. The concept of spin-wave renormalization, which we will apply, allows the spin-wave energies to have a temperature dependence such that these energies more closely resemble the energies of the true collective modes which may be excited at a given temperature. Since we wish to provide some experimental verification for the approximations used in spin-wave renormalization, it is necessary to follow the spin system from low temperatures up to about $T_c/2$. It has been observed[10] that the anisotropy field for $CrBr_3$ decreased by about 30% over this temperature range; this variation must be taken into account by any precise theory.

After introducing angular momentum raising and lowering operators

$$\begin{aligned}R_k{}^{\pm}&=R_k{}^x\pm iR_k{}^y,\\S_j{}^{\pm}&=S_j{}^x\pm iS_j{}^y,\end{aligned}\quad(2.2)$$

we make the following transformation to boson operators[11–13]:

$$\begin{aligned}S_j{}^z&=S-a_j{}^\dagger a_j,\\S_j{}^-&=(2S)^{1/2}a_j{}^\dagger,\\S_j{}^+&=(2S)^{1/2}[a_j-a_j{}^\dagger a_ja_j/(2S)],\\R_k{}^z&=S-b_k{}^\dagger b_k,\\R_k{}^-&=(2S)^{1/2}b_k{}^\dagger,\\R_k{}^+&=(2S)^{1/2}[b_k-b_k{}^\dagger b_kb_k/(2S)].\end{aligned}\quad(2.3)$$

When the a_j and b_k operators satisfy the boson commutation relations

$$\begin{aligned}&[b_k,b_{k'}{}^\dagger]=\delta_{kk'},\quad[a_j,a_{j'}{}^\dagger]=\delta_{jj'},\\&[b_k{}^\dagger,b_{k'}{}^\dagger]=[b_k,b_{k'}]=[a_j{}^\dagger,a_{j'}{}^\dagger]=[a_j,a_{j'}]=0,\\&[b_k{}^\dagger,a_j{}^\dagger]=[b_k,a_j]=[b_k,a_j{}^\dagger]=[b_k{}^\dagger,a_j]=0,\end{aligned}\quad(2.4)$$

the angular momentum operators $\mathbf{R}_k$ and $\mathbf{S}_j$ satisfy the usual angular momentum commutation relations. Using (2.2) and (2.3), we obtain Dyson's[14] ideal spin-wave Hamiltonian for our $CrBr_3$ model:

$$\begin{aligned}\mathcal{H}=&E_0+[g\mu_BH_A(T)+6J_TS+4J_LS]\\&\times(\textstyle\sum_j a_j{}^\dagger a_j+\sum_k b_k{}^\dagger b_k)\\&-2J_TS\textstyle\sum_{j,\delta}(b_{j+\delta}{}^\dagger a_j+a_j{}^\dagger b_{j+\delta})\\&-2J_LS(\textstyle\sum_{j,\delta'}a_{j+\delta'}{}^\dagger a_j+\sum_{k,\delta'}b_{k+\delta'}{}^\dagger b_k)\\&-2J_T\textstyle\sum_{j,\delta}a_j{}^\dagger a_jb_{j+\delta}{}^\dagger b_{j+\delta}\\&+J_L\textstyle\sum_{j,\delta'}(a_{j+\delta'}{}^\dagger a_j{}^\dagger a_ja_j-a_j{}^\dagger a_ja_{j+\delta'}{}^\dagger a_{j+\delta'})\\&+J_L\textstyle\sum_{k,\delta'}(b_{k+\delta'}{}^\dagger b_k{}^\dagger b_kb_k-b_k{}^\dagger b_kb_{k+\delta'}{}^\dagger b_{k+\delta'})\\&+J_T\textstyle\sum_{j,\delta}(b_{j+\delta}{}^\dagger a_j{}^\dagger a_ja_j+a_j{}^\dagger b_{j+\delta}{}^\dagger b_{j+\delta}b_{j+\delta}),\end{aligned}\quad(2.5)$$

with

$$E_0=-6J_TS^2N-4J_LS^2N-2g\mu_BH_A(T)SN.\quad(2.6)$$

Following standard spin-wave theories, we introduce the Fourier transformations:

$$\begin{aligned}a_j&=N^{-1/2}\textstyle\sum_\lambda\exp(-i\mathbf{j}\cdot\boldsymbol{\lambda})a_\lambda,\\a_j{}^\dagger&=N^{-1/2}\textstyle\sum_\lambda\exp(i\mathbf{j}\cdot\boldsymbol{\lambda})a_\lambda{}^\dagger,\\b_k&=N^{-1/2}\textstyle\sum_\lambda\exp(-i\mathbf{k}\cdot\boldsymbol{\lambda})b_\lambda,\\b_k{}^\dagger&=N^{-1/2}\textstyle\sum_\lambda\exp(i\mathbf{k}\cdot\boldsymbol{\lambda})b_\lambda{}^\dagger,\end{aligned}\quad(2.7)$$

where the sums are taken over the first Brillouin zone of the reciprocal lattice of a sublattice. From (2.4) it is seen that the a_λ and b_λ also obey boson commutation relations

$$\begin{aligned}&[a_\lambda,a_\mu{}^\dagger]=[b_\lambda,b_\mu{}^\dagger]=\delta_{\lambda\mu},\\&[a_\lambda,a_\mu]=[a_\lambda{}^\dagger,a_\mu{}^\dagger]=[b_\lambda,b_\mu]=[b_\lambda{}^\dagger,b_\mu{}^\dagger]=0,\end{aligned}\quad(2.8)$$

with the a_λ, $a_\lambda{}^\dagger$ operators commuting with the b_μ, $b_\mu{}^\dagger$ operators. Using (2.7) in (2.5)

$$\mathcal{H}=\mathcal{H}_0+\mathcal{H}_1,\quad(2.9)$$

where

$$\begin{aligned}\mathcal{H}_0=&E_0+\textstyle\sum_\lambda[g\mu_BH_A(T)+6J_TS+4J_LS(1-\gamma_\lambda')]\\&\times(a_\lambda{}^\dagger a_\lambda+b_\lambda{}^\dagger b_\lambda)-6J_TS\textstyle\sum_\lambda(\gamma_\lambda b_\lambda{}^\dagger a_\lambda+\gamma_{-\lambda}a_\lambda{}^\dagger b_\lambda),\end{aligned}\quad(2.10)$$

with

$$\gamma_\lambda=\tfrac{1}{3}\textstyle\sum_\delta\exp(i\boldsymbol{\lambda}\cdot\boldsymbol{\delta}),\quad(2.11)$$

and

$$\gamma_\lambda'=\tfrac{1}{2}\textstyle\sum_{\delta'}\exp(i\boldsymbol{\lambda}\cdot\boldsymbol{\delta}'),\quad(2.12)$$

[10] J. F. Dillon, J. Appl. Phys. Suppl. **33**, 1191S (1962).
[11] S. V. Maleev, Zh. Eksperim. i Teor. Fiz. **33**, 1010 (1957) [English transl.: Soviet Phys.—JETP **6**, 776 (1958)].
[12] R. A. Tahir-Kheli and D. ter Haar, Phys. Rev. **127**, 95 (1962).
[13] T. Oguchi, Progr. Theoret. Phys. (Kyoto) **25**, 721 (1961).
[14] F. J. Dyson, Phys. Rev. **102**, 1217, 1230 (1956).

while

$$\mathcal{H}_1=N^{-1}\sum_{\lambda_1,\cdots,\lambda_4}\delta(\lambda_1+\lambda_2-\lambda_3-\lambda_4)$$
$$\times[2J_L(\gamma_1'-\gamma_{2-4}')a_1^\dagger a_2^\dagger a_3 a_4$$
$$+2J_L(\gamma_1'-\gamma_{2-4}')b_1^\dagger b_2^\dagger b_3 b_4-6J_T\gamma_{2-4}a_1^\dagger b_2^\dagger a_3 b_4$$
$$+3J_T\gamma_1 b_1^\dagger a_2^\dagger a_3 a_4+3J_T\gamma_{-1}a_1^\dagger b_2^\dagger b_3 b_4]. \quad (2.13)$$

Above we have used the notation a_1, γ_1, etc., instead of a_{λ_1}, γ_{λ_1}, etc.; such notation will also be used later in the paper.

The diagonalization of $\mathcal{H}_0$ is achieved by applying the transformation

$$\begin{aligned}a_\lambda&=2^{-1/2}\exp(i\theta_\lambda)(\alpha_\lambda+\beta_\lambda),\\ a_\lambda^\dagger&=2^{-1/2}\exp(-i\theta_\lambda)(\alpha_\lambda^\dagger+\beta_\lambda^\dagger),\\ b_\lambda&=2^{-1/2}\exp(-i\theta_\lambda)(\alpha_\lambda-\beta_\lambda),\\ b_\lambda^\dagger&=2^{-1/2}\exp(i\theta_\lambda)(\alpha_\lambda^\dagger-\beta_\lambda^\dagger),\end{aligned} \quad (2.14)$$

with

$$\exp(4i\theta_\lambda)=\gamma_{-\lambda}/\gamma_\lambda. \quad (2.15)$$

Using (2.14) and (2.8), it is seen that the α and β operators satisfy boson commutation relations:

$$\begin{aligned}&[\alpha_\lambda,\alpha_\mu^\dagger]=[\beta_\lambda,\beta_\mu^\dagger]=\delta_{\lambda\mu},\\ &[\alpha_\lambda,\alpha_\mu]=[\alpha_\lambda^\dagger,\alpha_\mu^\dagger]=[\beta_\lambda,\beta_\mu]=[\beta_\lambda^\dagger,\beta_\mu^\dagger]=0,\end{aligned} \quad (2.16)$$

with the α_λ, $\alpha_\lambda^\dagger$ operators commuting with the β_μ, $\beta_\mu^\dagger$ operators. Using the transformation (2.14) $\mathcal{H}_0$ goes over to its diagonal form

$$\mathcal{H}_0=E_0+\sum_\lambda\{g\mu_B H_A(T)+6J_T S[1-(\gamma_\lambda\gamma_{-\lambda})^{1/2}]$$
$$+4J_L S(1-\gamma_\lambda')\}\alpha_\lambda^\dagger\alpha_\lambda+\sum_\lambda\{g\mu_B H_A(T)$$
$$+6J_T S[1+(\gamma_\lambda\gamma_{-\lambda})^{1/2}]+4J_L S(1-\gamma_\lambda')\}\beta_\lambda^\dagger\beta_\lambda. \quad (2.17)$$

The quasiparticles represented by (2.17) are HP type spin waves and are the usual approximate collective modes utilized when one is working at *low* temperatures; i.e., $\mathcal{H}_1$ is usually neglected at low temperatures. Another common approximation made when using (2.17) is the long-wavelength approximation, which consists of expanding the lower branch of the dispersion law in a series in powers of λ and retaining only the first term which goes as λ^2.

In Sec. IV we will investigate both the long-wavelength approximation and the neglect of $\mathcal{H}_1$. In order to investigate the effect of the long-wavelength approximation on the calculated magnetization, we will perform the required integration over the first Brillouin zone numerically for both spin-wave branches. However, investigation of the effect of neglecting $\mathcal{H}_1$ is not so simple. Since Dyson[14] has shown for the cubic lattices that the kinematic interaction may be neglected at reasonable temperatures, we will assume that the kinematic interaction may be neglected in our treatment of $CrBr_3$. Furthermore, as suggested by Kittel[15] and verified by Bloch[7] for the simple cubic lattice up to at least $T_c/2$, Dyson's results indicate that spin-wave spin-wave interactions in ferromagnets may be relatively weak in this temperature range. In Bloch's treatment, interactions were taken into account by renormalization of the spin-wave energies. Her renormalization was performed by assuming that all nondiagonal terms of the Hamiltonian could be neglected. This approximation allowed her to obtain reasonable values of T_c for the simple cubic lattice. Thus, one would expect the neglect of the nondiagonal terms of the Hamiltonian to be valid up to, say, at least $T_c/2$. Therefore, in our treatment of $CrBr_3$ we will restrict ourselves to that range and retain only that portion of $\mathcal{H}_1$ which is diagonal in the α, β representation. The portion of $\mathcal{H}_1$ so retained will be accounted for in the theory by applying a renormalization procedure.

The part of $\mathcal{H}_1$ which is diagonal in the α, β representation is

$$\mathcal{H}_{1d}=-N^{-1}\textstyle\sum_{\lambda_1,\lambda_2}[(3J_T/2)\{1+\gamma_{2-1}\exp[2i(\theta_2-\theta_1)]$$
$$-(\gamma_1\gamma_{-1})^{1/2}-(\gamma_2\gamma_{-2})^{1/2}\}$$
$$+J_L(1-\gamma_1')(1-\gamma_2')]\alpha_1^\dagger\alpha_1\alpha_2^\dagger\alpha_2$$
$$-N^{-1}\textstyle\sum_{\lambda_1,\lambda_2}[(3J_T/2)\{1+\gamma_{2-1}\exp[2i(\theta_2-\theta_1)]$$
$$+(\gamma_1\gamma_{-1})^{1/2}+(\gamma_2\gamma_{-2})^{1/2}\}$$
$$+J_L(1-\gamma_1')(1-\gamma_2')]\beta_1^\dagger\beta_1\beta_2^\dagger\beta_2$$
$$-N^{-1}\textstyle\sum_{\lambda_1,\lambda_2}[3J_T\{1+(\gamma_2\gamma_{-2})^{1/2}-(\gamma_1\gamma_{-1})^{1/2}$$
$$-(1/2)\gamma_{2-1}\exp[2i(\theta_2-\theta_1)]$$
$$-(1/2)\gamma_{1-2}\exp[2i(\theta_1-\theta_2)]\}$$
$$+2J_L(1-\gamma_1')(1-\gamma_2')]\alpha_1^\dagger\alpha_1\beta_2^\dagger\beta_2. \quad (2.18)$$

The total Hamiltonian which we are now retaining for our treatment is

$$\mathcal{H}_d=\mathcal{H}_0+\mathcal{H}_{1d}. \quad (2.19)$$

We now apply a renormalization procedure to the system described by $\mathcal{H}_d$, The procedure we use is different from the one used by Bloch but the results would be the same. Spin-wave renormalization is accomplished here by applying the exact relation[16,17]

$$\{[\mathcal{H}_d,\theta_\lambda^\dagger]-\epsilon_\lambda\theta_\lambda^\dagger\}\Psi=0, \quad (2.20)$$

where $\theta_\lambda^\dagger$ is the creation operator for a true collective mode of $\mathcal{H}_d$; Ψ is *any* eigenstate of the system, and ϵ_λ the energy required to excite, above Ψ, a collective mode of wave number λ. In our theory, we will approximate $\theta_\lambda^\dagger$ by either $\alpha_\lambda^\dagger$ or $\beta_\lambda^\dagger$ depending on the dispersion branch of interest; then, after performing the commutator $[\mathcal{H}_d,\theta_\lambda^\dagger]$, we will replace number operators by their thermal expectation values. That is, we assume that the Ψ of (2.20) is not an eigenstate of the system but a state which has expectation values for the number

[15] C. Kittel, International Conference on Magnetic Relaxation, Eindhoven, July, 1962 (unpublished).
[16] H. Suhl and N. R. Werthamer, Phys. Rev. **122**, 359 (1961).
[17] J. Korringa, Phys. Rev. **125**, 1972 (1962).

operators equal to the thermal expectation values at a given temperature T. This assumption gives the same renormalization results as the method used by Bloch[7]; but we prefer using the relation (2.20) because it leads to a physical interpretation of why renormalization must exist. Also, by use of (2.20) it is readily apparent how higher orders of the renormalization procedure could be derived; i.e., one would use the entire Hamiltonian instead of just $\mathcal{H}_d$ and approximate $\theta_\lambda^\dagger$ by a sum of one operator terms, three operator terms, etc., as Korringa[17] has done in his investigation of single excitations above the ground state of an antiferromagnet. Using the above method, we obtain the following first-order energy for the lower branch (lower sign) and the upper branch (upper sign):

$$\begin{aligned}\epsilon_{\lambda_1}^{\pm}(T)=&\{g\mu_B H_A(T)+6J_T S[1\pm(\gamma_1\gamma_{-1})^{1/2}]\\&+4J_L S(1-\gamma_1')\}-(3J_T/N)\\&\times\textstyle\sum_{\lambda_2}\{1\mp(1/2)\gamma_{2-1}\exp[2i(\theta_2-\theta_1)]\\&\mp(1/2)\gamma_{1-2}\exp[2i(\theta_1-\theta_2)]\\&\pm(\gamma_1\gamma_{-1})^{1/2}-(\gamma_2\gamma_{-2})^{1/2}\}\langle\alpha_2^\dagger\alpha_2\rangle\\&-(3J_T/N)\textstyle\sum_{\lambda_2}\{1\pm(1/2)\gamma_{2-1}\exp[2i(\theta_2-\theta_1)]\\&\pm(1/2)\gamma_{1-2}\exp[2i(\theta_1-\theta_2)]\\&\pm(\gamma_1\gamma_{-1})^{1/2}+(\gamma_2\gamma_{-2})^{1/2}\}\langle\beta_2^\dagger\beta_2\rangle\\&-(2J_L/N)(1-\gamma_1')\textstyle\sum_{\lambda_2}(1-\gamma_2')\\&\times[\langle\alpha_2^\dagger\alpha_2\rangle+\langle\beta_2^\dagger\beta_2\rangle].\end{aligned}\tag{2.21}$$

In the above the excitations are pure bosons, since we are neglecting the kinematic interaction, giving

$$\langle\alpha_\lambda^\dagger\alpha_\lambda\rangle=\{\exp[\epsilon_\lambda^-(T)/kT]-1\}^{-1},\tag{2.22}$$

and

$$\langle\beta_\lambda^\dagger\beta_\lambda\rangle=\{\exp[\epsilon_\lambda^+(T)/kT]-1\}^{-1}.\tag{2.23}$$

A numerical solution of (2.21) through (2.23) for $\epsilon_\lambda^-(T)$ and $\epsilon_\lambda^+(T)$ would be extremely tedious, if not impossible when varying J_T and J_L to fit data, because of the

$$(3J_T/N)\textstyle\sum_{\lambda_2}\gamma_{2-1}\exp[2i(\theta_2-\theta_1)]\langle\alpha_2^\dagger\alpha_2\rangle\tag{2.24}$$

type of terms. It is therefore necessary to investigate this term and obtain some simplification. Rewriting (2.24) using (2.11) and (2.15) gives

$$\begin{aligned}&(3J_T/2N)(\gamma_1/\gamma_{-1})^{1/2}\tfrac{1}{3}\textstyle\sum_\delta\exp(-i\boldsymbol{\delta}\cdot\boldsymbol{\lambda}_1)\\&\times[\textstyle\sum_{\lambda_2}\exp(i\boldsymbol{\delta}\cdot\boldsymbol{\lambda}_2)(\gamma_{-2}/\gamma_2)^{1/2}\langle\alpha_2^\dagger\alpha_2\rangle].\end{aligned}\tag{2.25}$$

Due to the symmetry of the crystal, the $\epsilon^\pm(T)$, and hence $\langle\alpha_\lambda^\dagger\alpha_\lambda\rangle$ and $\langle\beta_\lambda^\dagger\beta_\lambda\rangle$, must contain the $\boldsymbol{\delta}$ in a symmetrical fashion; thus, each term in the [ ] brackets in (2.25) is equal for each of the $\boldsymbol{\delta}$. So (2.25) goes over to

$$(3J_T/N)(\gamma_1\gamma_{-1})^{1/2}\textstyle\sum_{\lambda_2}(\gamma_2\gamma_{-2})^{1/2}\langle\alpha_2^\dagger\alpha_2\rangle.\tag{2.26}$$

Using (2.26) and similar relations, the approximate renormalized energies are

$$\begin{aligned}\epsilon_\lambda^{\pm}(T)=&g\mu_B H_A(T)+6J_T S\xi_1(T)[1\pm(\gamma_\lambda\gamma_{-\lambda})^{1/2}]\\&+4J_L S\xi_2(T)(1-\gamma_\lambda'),\end{aligned}\tag{2.27}$$

where

$$\begin{aligned}\xi_1(T)=1-(1/2SN)\textstyle\sum_\mu\{&\langle\alpha_\mu^\dagger\alpha_\mu\rangle[1-(\gamma_\mu\gamma_{-\mu})^{1/2}]\\&+\langle\beta_\mu^\dagger\beta_\mu\rangle[1+(\gamma_\mu\gamma_{-\mu})^{1/2}]\},\end{aligned}\tag{2.28}$$

and

$$\xi_2(T)=1-(1/2SN)\textstyle\sum_\mu(1-\gamma_\mu')[\langle\alpha_\mu^\dagger\alpha_\mu\rangle+\langle\beta_\mu^\dagger\beta_\mu\rangle].\tag{2.29}$$

The two implicit equations (2.28) and (2.29) may now be solved for $\xi_1(T)$ and $\xi_2(T)$ as functions of T by using an iterative procedure. Details of their numerical solution will be given in Sec. IV. The calculation of the magnetization of the crystal is then straightforward, using standard methods, once $\xi_1(T)$ and $\xi_2(T)$ are obtained. The magnetization as a function of T is given by

$$M(T)=M(0)[1-(1/2NS)\textstyle\sum_\lambda(\langle\alpha_\lambda^\dagger\alpha_\lambda\rangle+\langle\beta_\lambda^\dagger\beta_\lambda\rangle)].\tag{2.30}$$

III. EXPERIMENTAL PROCEDURES

The zero-field Cr^{53} nuclear resonances were observed with a push-pull FM marginal oscillator[18] followed by a conventional synchronous detection system. Oscillator frequencies were measured with a digital counter. The nuclear resonances reported here arise from Cr^{53} nuclei situated in the ferromagnetic domains of $CrBr_3$. The splitting between the satellites of the quadrupole triplet was found to be 590 ± 4 kc/sec, independent of temperature. The experimental frequencies given in Table I correspond to the $\frac{1}{2}\leftrightarrow-\frac{1}{2}$ transition.

Samples were prepared by slow vacuum sublimation (800°C) of material obtained from the high-temperature bromination of 99.99% chromium metal. The sublimation product consisted of large ($\sim\frac{1}{4}$ in. diam) but very thin flakes. These flakes were carefully loaded into flat-bottomed Lucite sample holders of ~3 cm^3 volume.

Temperatures of 1–4 and 14–20°K were obtained with liquid-helium and liquid- (equilibrium) hydrogen baths, respectively. Constant temperatures were maintained by regulating the bath pressure with a manostat. Temperature measurements were based on the appropriate vapor-pressure scales. In the temperature range 4–14°K the sample was contained in a vacuum-jacketed heat-leak chamber which was immersed in a 4°K He bath. In this range the sample temperature was measured with germanium resistance thermometers[19] and temperature regulation was achieved by manual control of the power input to a heater. The germanium thermometers were calibrated by us against the ac magnetic susceptibility of chromium-methylammonium alum. Our temperature measurements have an estimated maximum error of 0.01°K below 4°K and 0.02°K above 4°K.

IV. NUMERICAL RESULTS

In Sec. II we have discussed a renormalization procedure, leading to a relation for the magnetization of

[18] R. G. Shulman, Phys. Rev. **121**, 125 (1961).
[19] Texas Instruments, Inc., Type 104-A.

TABLE I. A comparison of the experimental results and the best theoretical fit obtained in the present investigation for the Cr^{53} NMR zero-field frequencies. The best theoretical fit is for a renormalized spin-wave theory with $J_T/k=8.25°K$, $J_L/k=0.497°K$, $\nu(0)=58.099$ Mc/sec, and a temperature-dependent anisotropy as explained in the text. The difference between theory and experiment gives a rms deviation of 16.2 kc/sec. $\xi_1(T)$ is the intralayer renormalization constant, and $\xi_2(T)$ the interlayer renormalization constant.

T(°K)	Experiment (Mc/sec)	Best theory (Mc/sec)	Theory minus experiment (kc/sec)	$\xi_1(T)$	$\xi_2(T)$
1.44	58.032	58.036	4	1.0000	1.0000
1.58	58.016	58.020	4	1.0000	0.9998
1.74	57.993	57.999	6	1.0000	0.9996
1.86	57.978	57.983	5	1.0000	0.9994
2.01	57.956	57.960	4	1.0000	0.9992
2.31	57.905	57.910	5	1.0000	0.9988
2.66	57.837	57.842	5	0.9999	0.9982
3.17	57.719	57.728	9	0.9998	0.9970
4.02	57.497	57.501	4	0.9996	0.9946
4.05	57.491	57.493	2	0.9996	0.9945
4.12	57.471	57.472	1	0.9996	0.9942
4.36	57.402	57.399	−3	0.9995	0.9934
4.57	57.336	57.332	−4	0.9994	0.9926
4.90	57.226	57.223	−3	0.9993	0.9913
4.94	57.214	57.210	−4	0.9992	0.9912
5.25	57.113	57.102	−11	0.9991	0.9898
5.58	56.978	56.983	5	0.9989	0.9884
5.91	56.860	56.858	−2	0.9987	0.9868
6.14	56.767	56.768	1	0.9986	0.9857
6.67	56.553	56.553	0	0.9982	0.9830
6.97	56.430	56.425	−5	0.9980	0.9813
7.50	56.198	56.191	−7	0.9975	0.9783
7.98	55.993	55.969	−24	0.9970	0.9753
8.30	55.837	55.816	−21	0.9967	0.9733
8.75	55.610	55.594	−16	0.9962	0.9703
8.87	55.554	55.534	−20	0.9961	0.9695
9.17	55.391	55.381	−10	0.9957	0.9675
9.63	55.158	55.139	−19	0.9951	0.9642
9.92	54.944	54.984	40	0.9947	0.9621
10.20	54.832	54.828	−4	0.9943	0.9599
10.73	54.544	54.524	−20	0.9935	0.9558
11.08	54.295	54.319	24	0.9929	0.9530
11.16	54.257	54.271	14	0.9928	0.9523
11.64	53.969	53.979	10	0.9919	0.9483
11.91	53.789	53.812	23	0.9914	0.9460
12.13	53.661	53.673	12	0.9910	0.9440
12.54	53.386	53.411	25	0.9902	0.9404
12.90	53.156	53.176	20	0.9895	0.9371
13.22	52.943	52.963	20	0.9888	0.9341
13.34	52.873	52.882	9	0.9885	0.9330
13.69	52.651	52.643	−8	0.9877	0.9296
14.00	52.435	52.429	−6	0.9870	0.9266
14.09	52.374	52.366	−8	0.9868	0.9257
14.60	52.010	52.005	−5	0.9856	0.9206
15.06	51.680	51.670	−10	0.9844	0.9159
15.44	51.382	51.389	7	0.9834	0.9119
15.93	51.046	51.018	−28	0.9820	0.9066
16.59	50.548	50.506	−42	0.9801	0.8993
17.13	50.102	50.085	−17	0.9783	0.8925
17.58	49.732	49.711	−21	0.9771	0.8879
18.07	49.299	49.303	4	0.9754	0.8820
18.80	48.696	48.680	−16	0.9729	0.8730
19.17	48.370	48.357	−13	0.9716	0.8684
19.68	47.856	47.905	49	0.9697	0.8618

$CrBr_3$, which, we feel, should be reasonably accurate up to about one-half the Curie temperature. The theory developed there will now be used to interpret the experimental results of the preceding section. First, the relations (2.28) and (2.29) for the renormalization constants are written in a form more suitable for numerical evaluation by changing the sums to integrals over the first Brillouin zone; also, a change of variables has been made and S set equal to $\frac{3}{2}$, its value for the $CrBr_3$ case:

$$\xi_1(T)=1-(4/72\pi^3)\int_0^{2\pi}dy\int_0^{4\pi-y}dx\int_0^{\pi}dz \times\{[1-f(x,y)]\{\exp[\epsilon^-(x,y,z)/kT]-1\}^{-1} +[1+f(x,y)]\{\exp[\epsilon^+(x,y,z)/kT]-1\}^{-1}\}, \quad (4.1)$$

and

$$\xi_2(T)=1-(4/72\pi^3)\int_0^{2\pi}dy\int_0^{4\pi-y}dx\int_0^{\pi}dz(1-\cos z) \times\{\{\exp[\epsilon^-(x,y,z)/kT]-1\}^{-1} +\{\exp[\epsilon^+(x,y,z)/kT]-1\}^{-1}\}, \quad (4.2)$$

where

$$\epsilon^{\pm}(x,y,z)=g\mu_B H_A(T)+9J_T\xi_1(T)[1\pm f(x,y)] +6J_L\xi_2(T)[1-\cos z], \quad (4.3)$$

and

$$f(x,y)=\tfrac{1}{3}[3+4\cos(x/6)\cos(y/2)+2\cos(x/3)]^{1/2}. \quad (4.4)$$

These equations, for a given T, J_T, and J_L set, were solved for $\xi_1(T)$ and $\xi_2(T)$ by the following iterative process. First, we assumed a value for $\xi_2(T)$ (≤ 1 depending upon any prior knowledge about the T, J_T, and J_L set), and then solved (4.1) for $\xi_1(T)$; this value for $\xi_1(T)$ was then used to solve (4.2) for $\xi_2(T)$, which was then used to solve (4.1) for $\xi_1(T)$, etc. The iterative process was terminated when both $\xi_1(T)$ and $\xi_2(T)$ were found to be consistent within ± 0.0005. At any given step of the process there were two roots for $\xi_i(T)$; however, we have restricted ourselves to the root which makes the renormalization process continuous with HP spin-wave theory at low temperatures. The theoretical NMR frequency $\nu(T)$ for a given T, J_T, and J_L set is then calculated by using the self-consistent $\xi_1(T)$, $\xi_2(T)$ set in

$$\nu(T)=\nu(0)\Big[1-(4/72\pi^3)\int_0^{2\pi}dy\int_0^{4\pi-y}dx\int_0^{\pi}dz \times\{\{\exp[\epsilon^-(x,y,z)/kT]-1\}^{-1} +\{\exp[\epsilon^+(x,y,z)/kT]-1\}^{-1}\}\Big], \quad (4.5)$$

which is obtained from (2.30) by assuming the hyperfine coupling constant of the Cr^{3+} ion does not appreciably change over the temperature range for our experimental results of Table I. Although $\nu(0)=58.096\pm 0.010$ Mc/sec was previously determined[2] by extrapolation of the experimental data, we will vary $\nu(0)$ within the error limits in the present investigation in attempting least-squares fits to the data.

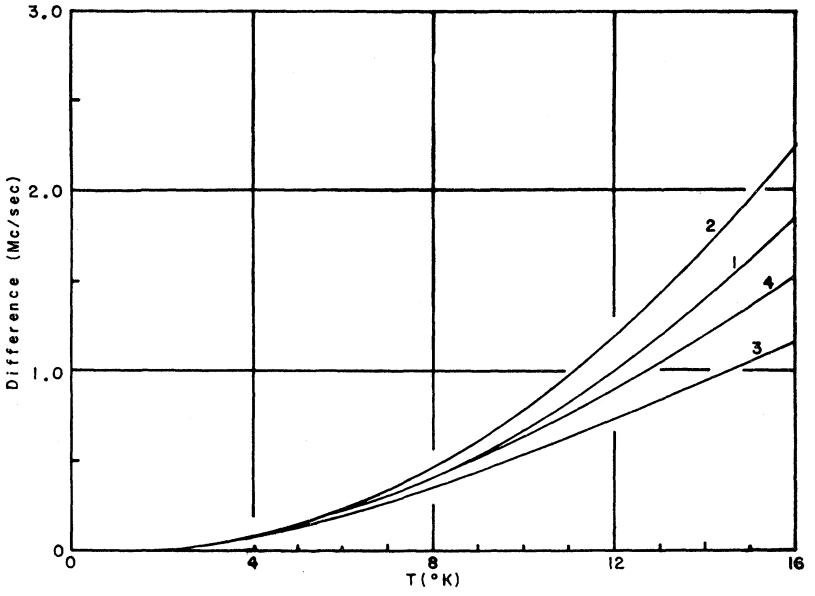

FIG. 2. The difference between experimental and theoretical Cr^{53} NMR zero-field frequencies as a function of temperature using $J_T/k = 5.44°K$, $J_L/k = 0.88°K$, and $\nu(0) = 58.096$ Mc/sec. Curves 1 and 2 are for a renormalized spin-wave theory with, respectively, $H_A(T) = 6850$ Oe independent of temperature, and $H_A(T)$ having the temperature variation explained in the text. Curves 3 and 4 are for HP spin-wave theory with, respectively, $H_A(T)$ as in 1 and 2.

In fitting their data, GJR not only neglected $\mathcal{H}_1$ but also used only the lower spin-wave branch in their calculations; furthermore, they adopted the long-wavelength approximation for the transverse excitations to obtain a theoretical expression for the magnetization. In this manner, they obtained a series expansion in T for the magnetization with the leading temperature-dependent term going as $T^{3/2}$, as for a typical three-dimensional Heisenberg ferromagnet. Their justification for this procedure was probably that the magnetization data went approximately as $T^{3/2}$, with the observed deviation from the $T^{3/2}$ law being explainable by the $T^{5/2}$ term and by the exponential weighting factors containing the anisotropy. By restricting their analysis to the $T^{3/2}$ and $T^{5/2}$ terms, weighted by the exponential factors, they were able to fit their data and obtain values for J_T and J_L. As mentioned in Sec. I, we have had some doubt about the accuracy of the resulting exchange constants; thus, we want to investigate the approximations used in their treatment. In the following, we are going to investigate both the long-wavelength approximation and the neglect of $\mathcal{H}_1$.

In some of our calculations we have explicitly considered the temperature variation of the anisotropy given by $H_A(T) = 2K(T)/M(T)$. The anisotropy constant $K(T)$ was obtained from the measurements of Dillon,[10] while the magnetization $M(T)$ was taken from the experimental NMR data obtained in the present investigation. From the graph given by Dillon we obtained for $0°K \leq T \leq 10°K$

$$K(T)\times 10^{-5}\ (\text{erg/cm}^3) = 9.56 - 0.104T - 0.0037T^2, \quad (4.6)$$

and for $10°K < T \leq 20°K$

$$K(T)\times 10^{-5}\ (\text{erg/cm}^3) = 11.05 - 0.29T. \quad (4.7)$$

For $M(T)$ we have taken

$$M(T) = M(0)\{1 - [\nu(0) - \nu(T)]/\nu(0)\}; \quad (4.8)$$

the $\nu(T)$ are the observed Cr^{53} zero-field NMR frequencies, and $M(0)$ was adjusted to give $H_A(0) = 6850$ Oe (the value used by GJR).

The first attempt to fit the experimental data with (4.1) through (4.5) was made with $J_T/k = 5.44°K$, $J_L/k = 0.88°K$, and $\nu(0) = 58.096$ Mc/sec, as previously given by GJR. Two cases were calculated using these parameters: (a) $H_A(T) = 6850$ Oe and constant throughout the temperature range; (b) $H_A(0) = 6850$ Oe and having a temperature variation as explained above. The difference between the experimental results and the theoretical values so calculated are given in Fig. 2 as curves 1 and 2, respectively. As is seen, this attempt to fit the intermediate temperature data led to absolutely no success. It was then decided to reinvestigate just the low-temperature data by using HP spin-wave theory [i.e., Eq. (4.5) with $\xi_1(T) = \xi_2(T) = 1$] but without invoking the long-wavelength approximation. Using the same J_T, J_L, $\nu(0)$, and cases (a) and (b) for $H_A(T)$, we obtained curves 3 and 4, respectively, of Fig. 2. For example, it was found here that the theoretical results for $T = 5.25°K$ were 133 kc/sec lower than experiment for $H_A(T)$ of case (a), and 153 kc/sec lower for $H_A(T)$ of case (b). Furthermore, for $T = 4.02°K$ and the same $J's$, theory was 56 kc/sec lower for case (a), and 67 kc/sec lower for case (b). To give an idea of the effect of renormalization at these temperatures, the renormalization process of Eqs. (4.1)–(4.5) would further lower the NMR frequencies by about 6 kc/sec at 5.25°K, and by about 2 kc/sec at 4.02°K.

It is seen from the preceding paragraph that the long-wavelength approximation introduces considerable error in trying to obtain exchange constants from experiment,

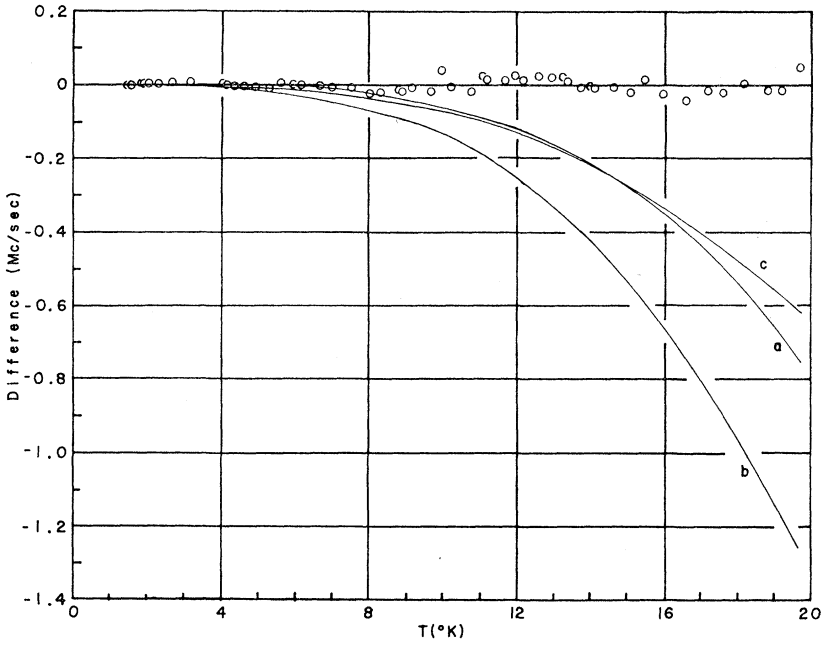

FIG. 3. The difference between the best theoretical fit and other theoretical Cr^{53} NMR zero-field frequencies as a function of temperature using $J_T/k=8.25°K$, $J_L/k=0.497°K$, and $\nu(0)=58.099$ Mc/sec. The best theoretical fit, represented by the abscissa, is for a renormalized spin-wave theory and a temperature dependent anisotropy as explained in the text. The experimental NMR frequencies are represented by the scatter about the abscissa. Curves a and b are for the HP spin-wave theory with, respectively, $H_A(T)$ having the temperature variation explained in the text, and $H_A(T)=6850$ Oe independent of temperature. Curve c is for a renormalized spin-wave theory with $H_A(T)=6850$ Oe independent of temperature.

even for temperatures of the order of $\frac{1}{6}$th the Curie temperature. Thus, our original doubt in the exchange constants quoted by GJR has been verified. To obtain exchange constants more descriptive of the Heisenberg model, it became necessary to refit the low-temperature data ($\leq 5.25°K$). This was done by first using HP spin-wave theory but applying minor renormalization corrections (0 to 6 kc/sec, depending on temperature) which remain constant over a wide range of the J's. Also, in this procedure we used $H_A(T)$ as described by (4.6)–(4.8). It was found that a fit to the data, within ± 10 kc/sec, could be obtained for $8.0°K \leq J_T/k \leq 9.7°K$ and with $0.536°K \geq J_L/k \geq 0.360°K$, depending on the value of J_T.

The higher temperature data were next included in the interpretation to see if the above range of J's would explain the data, thereby hoping to give some experimental verification of the approximations used in developing the renormalization theory of Sec. II. At the same time, it was hoped that the high temperature results would help narrow the range of the J's obtained at the lower temperatures. Using (4.1) through (4.5) and $H_A(T)$ as explained by (4.6)–(4.8), it was found that we could fit the entire temperature range of our data with an rms error of 16.2 kc/sec with $J_T/k=8.25°K$ and $J_L/k=0.497°K$. The rms error lies within our experimental uncertainty. It is to be emphasized that considerable[20] computer time was required to obtain this fit, and that an exhaustive least squares analysis in the neighborhood of these J's would therefore be prohibitive. However, using some selected temperatures, the J plane in the neighborhood of these values has been investigated, such that one can assign reasonable error limits to the J's. Our feeling is that for the $CrBr_3$ Heisenberg model described by (2.1) one must assign

$$\begin{aligned} &J_T/k=8.25\pm 0.10°K, \\ &J_L/k=0.497\mp 0.013°K, \\ &\nu(0)=58.099\pm 0.006 \text{ Mc/sec}. \end{aligned} \tag{4.9}$$

Thus, it is seen that using the intermediate-temperature data does help narrow the range of J's over which a theoretical fit to the experimental data can be obtained.

A comparison of the experimental data and the best theoretical fit, along with the $\xi_i(T)$'s obtained for such a fit, is given in Table I. From Fig. 3, where we have used the parameters of (4.9), one may see the effect of renormalization on the NMR frequency. The abscissa represents the best fit to the data, as described above, with the experimental points represented by scatter about the abscissa. Curve a represents the difference between the best fit and HP spin-wave theory with $H_A(T)$ having the temperature variation described by (4.6)–(4.8). Curve b is the deviation from the best fit for a HP spin-wave theory with $H_A(T)=6850$ Oe and constant with temperature. Finally, curve c represents the deviation from the best fit for a renormalized theory with $H_A(T)=6850$ Oe and constant with temperature.

V. DISCUSSION

The experimental determination of exchange parameters is of particular importance in the study of differences in magnetic properties of related compounds such as $CrCl_3$ and $CrBr_3$. In principle, the most accurate

[20] Approximately 20 h of a Control Data-1604 computer were required for the data reduction necessary for the present investigation.

method of determining these constants consists of the spin-wave analysis of magnetization data. Unfortunately, the theoretical fits which are obtained in this way often lack uniqueness if more than one parameter has to be determined. We have shown, for example, that the long-wavelength approximation to HP spin-wave theory is valid over such a limited temperature range that an accurate two parameter fit to the $CrBr_3$ data is impossible. A similar conclusion has been reached in the study of $CrCl_3$.[3] In the case of $CrBr_3$, even the exact application of HP spin-wave theory to the low-temperature measurements defines the appropriate exchange parameters only in an approximate way. The sensitivity of the theoretical fit can be improved by increasing the experimental accuracy or by extending the temperature range over which the theory is valid. In the present study we have taken the latter approach.

We have applied renormalization techniques to the calculation of the collective mode spectrum of the $CrBr_3$ spin system in order to take account of interactions between HP spin waves which are known to become important at sufficiently high temperatures. The resulting temperature-dependent spin-wave solution to the simple Heisenberg exchange Hamiltonian accurately accounts for our experimental observations over the range 1–20°K. We believe that the close agreement between theory and experiment provides strong justification for the approximations invoked in the renormalization procedure. By extending the experimental range to 20°K ($\sim T_c/2$) we have greatly reduced the uncertainty in the exchange parameters obtained from the NMR measurements.

The present method is quite adequate for the determination of two interaction constants for an exchange-coupled spin system. The extension to a greater number of unknown parameters, however, presently appears to be unfeasible. The computer time required to obtain a fit would become prohibitively lengthy. Moreover, the rapid loss of uniqueness in the fit which is expected to result from increasing the number of variables in the theory imposes a fundamental limitation on the amount of information which can be obtained from the measurement of a single magnetic property. In the present case, we were fortunate to have available an independent measurement of $H_A(0)$ and its temperature dependence. The application of the present techniques to obtain a single exchange parameter and $H_A(0)$ for $CrCl_3$ will be given elsewhere.[21]

The value of J_T obtained here for $CrBr_3$ is generally consistent with the known value of $T_c(37°K)$.[22] The nearly two-dimensional character of the $CrBr_3$ spin system combined with the low coordination number of its honeycomb lattice is expected to result in an unusually low T_c in relation to the exchange energy. For example, Brown and Luttinger[23] using the Kramers-Opechowski method have calculated transition temperatures (for $J/k=8.2°K$ and $S=\frac{3}{2}$) of approximately 37 and 33°K for the two-dimensional ferromagnetic triangular ($z=6$) and square ($z=4$) lattices, respectively. The honeycomb ($z=3$) lattice should yield an even lower value of T_c. The observed transition temperature is somewhat higher because of the presence of anisotropy and the weak interlayer coupling; it falls lower, however, than predicted by simple molecular-field theory (62°K). It appears that the present method is of particular value when the spin system has a pronounced one- or two-dimensional character. In cases of that type, application of the molecular-field model leads to large errors in the evaluation of the appropriate exchange constants. Examples, in addition to $CrBr_3$, are $CrCl_3$ which approximates a two-dimensional ferromagnet even more strongly than does $CrBr_3$, and perhaps $CuCl_2 \cdot 2H_2O$ which resembles a linear antiferromagnet.

ACKNOWLEDGMENTS

We are indebted to R. L. Rosenbaum for collecting most of the experimental data and to J. E. Hesse for preparation of the $CrBr_3$ samples. The least-squares analysis of the data was capably performed by Marcella M. Madsen.

---

[21] H. L. Davis and A. Narath, Phys. Rev. (to be published).
[22] I. Tsubokawa, J. Phys. Soc. Japan **15**, 1664 (1960).
[23] H. A. Brown and J. M. Luttinger, Phys. Rev. **100**, 685 (1955); H. A. Brown, *ibid.* **104**, 624 (1956).